Thermal Neutron Measurement Capability of a Single Crystal CVD Diamond Detector near the Reactor Core Region of UTR-KINKI[*]

Makoto I. KOBAYASHI[1,2], Sachiko YOSHIHASHI[3], Hirokuni YAMANISHI[4],
Siriyaporn SANGAROON[1,5], Kunihiro OGAWA[1,2], Mitsutaka ISOBE[1,2],
Akira URITANI[3] and Masaki OSAKABE[1,2]

[1]*National Institute for Fusion Science, National Institutes of Natural Sciences, Toki, Gifu 509-5292, Japan*
[2]*The Graduate University for Advanced Studies, SOKENDAI, Toki, Gifu 509-5292, Japan*
[3]*Nagoya University, Nagoya, Aichi 464-8603, Japan*
[4]*Kindai University, Atomic Energy Research Institute, Osaka 577-8502, Japan*
[5]*Mahasarakham University, Thailand*

Thermal neutron flux evaluation using a single crystal diamond detector (SDD) was carried out in the core region of the UTR-KINKI reactor where a mixed radiation field by thermal and fast neutrons and gamma-ray exists. The pulse shape discrimination method to extract pulses with a rectangular shape as well as a wide pulse-width was established to exclude pulses induced by gamma-rays. The SDD, using a ^{6}LiF thermal neutron converter, is able to detect pulse events caused not only by fast neutrons but also by thermal neutrons through energy depositions into the diamond by energetic alpha and triton particles induced by thermal neutrons. Additionally, the SDD without the thermal neutron converter was used for the measurement of the energy deposition events only by fast neutrons. A comparison of the pulse counts of the SDD with or without the thermal neutron convertor deduced the energy deposition spectra by thermal neutrons. The thermal neutron flux in the core region of the UTR-KINKI reactor was evaluated to be 7.6×10^6 n cm^{-2} s^{-1} W^{-1} up to a reactor power of 1 W.

1. Introduction

A single crystal diamond (SCD) is an attractive material as a fast neutron detector [1, 2]. Therefore, the application of a single crystal diamond detector (SDD) has been of interest in fusion reactor development because of fast neutrons generated by D (deuterium) -T (tritium) fusion reactions. The monitoring of fast neutrons using the SDD is proposed for the control of burning plasma. Indeed, there are some reports where the neutron yield from the fusion plasma was monitored by the SDD [3–10].

The SDD can detect not only fast neutrons but also energetic charged particles such as alpha particles. A lithium foil put on the surface of the SDD can react with thermal neutrons to generate energetic alpha and triton particles. Then these energetic charged particles can be detected by the SDD. Therefore the usage of a thermal neutron converter like a lithium foil gives the SDD a capability of thermal neutron measurement. This capability is also important for a fusion reactor. A blanket of a fusion reactor works to produce tritium, therefore, the actual measure-

ment of the tritium breeding is essential to check the performance of the blanket.

Thanks to the fast and thermal neutron measurement capabilities of the SDD, as well as other advantages, the SDD is a promising neutron detector for fusion reactors. On the other hand, the neutron field in a fusion reactor will be associated with gamma-rays. Therefore the pulse shape discrimination (PSD) methods for eliminating pulses induced by gamma-rays have been developed [11]. Our previous PSD method successfully separated pulses induced by gamma-rays and energetic charged particles in the thermal neutron field [12]. However, the additional influence of fast neutrons will make discrimination difficult. In this study, an advanced PSD method was proposed which can work to evaluate the thermal neutron flux in the field with fast neutrons and gamma-rays. A benchmark experiment was conducted near the core region of the UTR-KINKI reactor where wide energy neutrons and gamma-rays co-exist [13–15]. The performance of this PSD method was also investigated as a function of reactor power.

2. Experimental

2.1 Pulse shapes induced by various radiations

Hole-electron pairs are generated in the SCD by radiation. Applying bias voltage on a surface of the SCD, the charge in the SCD drifts in the opposite direction to produce a current eventually, according to the Schockley-Ramo theorem [16, 17]. The pulse shape induced by the radiation depends on the distribution of hole-electron pairs in the SCD. In the case of energetic charged particles, the hole-electron pairs locally generate as point-like on the surface region of the SCD. On the other hand, those generated by gamma-ray irradiation distribute in the entire bulk of the SCD by electron scattering. As a result, rectangular and triangular shaped pulses can be obtained by the energetic charged particles and gamma-ray irradiation, respectively [10, 11, 18].

In the case of fast neutron irradiation, fast neutrons can interact with the entire bulk of the SCD to generate the hole-electron pairs through elastic collisions and nuclear reactions. Therefore distribution of the hole-electron pairs will be point-like at any position of the SCD. Because the pulse shape results from a charge drift to the surface electrodes on the SCD, there are various pulse width and shapes induced by fast neutrons. For example, a two-step like pulse is usually obtained when a fast neutron interacts in the bulk of the SCD [19]. This two-step like shaped pulse can be misjudged as a triangular shaped pulse in the measurement using a conventional data acquisition system with the previous PSD method [10]. On the other hand, an event where fast neutrons hit on the surface of the SCD results in a rectangular shape, as in the case of energetic charged particles. The rectangular shaped pulse from the event at the surface would hardly be induced by gamma-rays, because the distribution of hole-electron pairs by gamma-ray should not be point-like. For these characteristics of pulses induced by fast neutrons, events by the hits of fast neutron or energetic charged particles on the surface of the SCD, which should result in a rectangular shaped pulse, were extracted by the PSD method in this study, to eliminate the pulses induced by gamma-rays. Then pulses by fast neutrons were evaluated using the SDD without a thermal neutron converter (see section 2.4). Besides, the SDD with a thermal neutron convertor could measure the pulses induced not only by fast neutrons but also the energetic charged particles induced by thermal neutrons. Therefore, the count rate of the energetic charged particles was corrected by the count rate of SDD without the thermal neutron converter to evaluate the thermal neutron flux.

2.2 PSD method

As discussed in section 2.1, the rectangular shaped pulses will be extracted by the present PSD method. This PSD was conducted by the index of "rectangularity, R", which is a value to express how the pulse shape is close to
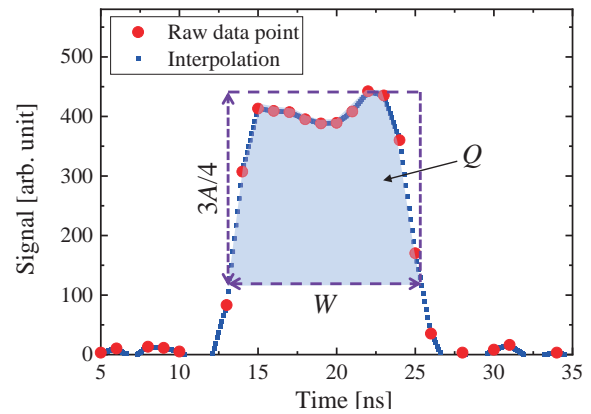

Fig. 1 Definition of R in PSD method. Blue colored area indicates Q. Therefore $R = 4Q/3AW$.

rectangular. The definition of R can be found in Fig. 1. The pulse induced by alpha-rays from [241]Am is displayed here as an example. The raw data points with the sampling rate of 1 GHz (explained in section 2.3) were interpolated by a spline function. Then the FW1/4PH (Full width of one-fourth of the peak height, W) and the peak height (A) were precisely evaluated. The rectangularity is the ratio of the charge exceeding one-fourth of the peak height (Q) to the area of the rectangular by W and $3A/4$. Therefore, R should be closed to unity when the pulse shape is rectangular.

2.3 Benchmark test using alpha and gamma-ray sources

The SDD (B6-C compact thermal-neutron diamond detector) from CIVIDEC Instrumentation GmbH was used [20]. The size and the thickness of the SCD were $4.5\,\mathrm{mm} \times 4.5\,\mathrm{mm}$, and $500\,\mu\mathrm{m}$, respectively. A 100 nm-thick titanium layer was on both SCD surfaces as metal electrodes. The signal from the SDD was transferred to a pre-amplifier (C2-HV broadband amplifier from CIVIDEC) [20]. The amplified signal was recorded by a DAQ system (APV8102-14MWPSAGb) composed of a fast processing ADC and FPGA system with a sampling rate of 1 GHz and resolution of 14 bit [21].

For pulse counting of the radiation sources, the [6]LiF thermal neutron converter was removed from the SDD. Therefore, radiation can directly access onto the SCD in the SDD. A 0.76 MBq ^{60}Co gamma-ray source and a ~550 Bq [241]Am alpha source were used. The alpha-ray source had a thin [241]Am layer deposited on the metal substrate. The pulse counting for these radiation sources was conducted separately. The distances between ^{60}Co and [241]Am sources were 10 cm and 2 mm from the SDD, respectively. A bias voltage of +250 V was applied to the detector for all the various measurements reported here after.

2.4 Radiation measurement in UTR-KINKI reactor

The same SDD as in section 2.3 was used. At this

time, the SDD was equipped with a 1.9 μm-thick ^{6}LiF thermal neutron converter with a ^{6}Li enrichment of 95%, and was inserted into the core region of the UTR-KINKI reactor through a sample insertion hole on the top shield of the reactor. The pulse counting was conducted for several minutes under the criticality of the reactor. The reactor power was changed to 0.01, 0.1 and 1 W in each measurement. Thereafter, the same measurements were carried out using the SDD without the thermal neutron converter.

3. Results and Discussion

Figure 2 shows the histogram of R in cases of alpha-ray and gamma-ray irradiations. R for alpha-ray irradiation is concentrated in a range of 0.60 - 0.85, although pulses can be found with $R < 0.60$ with a possibility of about 7% in total. Besides, an R of pulses by gamma-rays can be found in a range of 0.28 - 0.75. Due to the overlap of the distribution of R in these two cases, there would be a 15% miscounting of alpha/gamma pulses using only R.
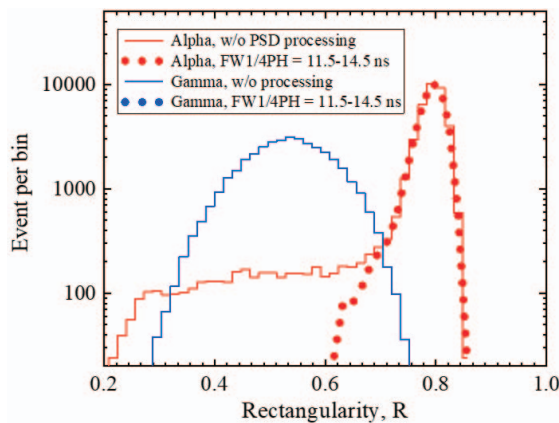

Fig. 2 Histogram of R in cases of alpha-ray and gamma-ray irradiation by ^{241}Am and ^{60}Co radiation source, respectively. Total pulse number in each case was 40000. Event rate of gamma pulse with wide FW1/4PH (blue dashed line) was less than lower limit of figure.
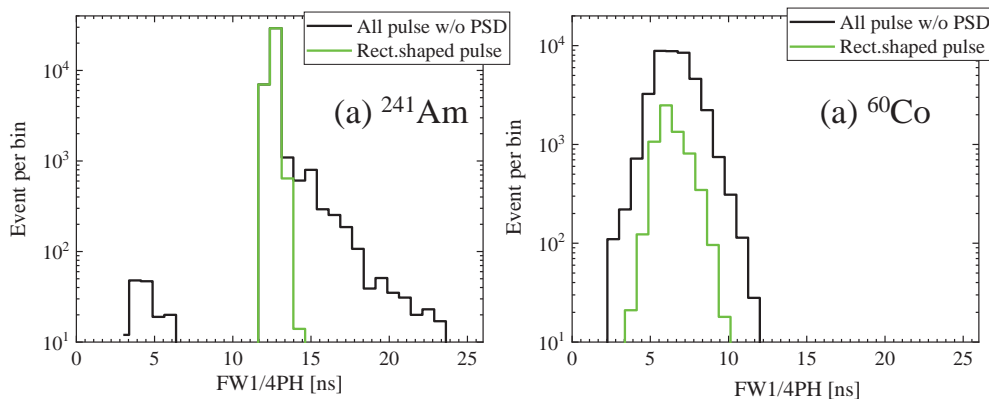
To improve discrimination capability, a parameter of FW1/4PH was also used. Figures 3 display a histogram of FW1/4PH for 40000 pulses during alpha or gamma-ray irradiation. In particular for alpha-ray irradiation, a sharp peak can be found for the pulses with rectangular shape in the FW1/4PH region of 11.5 - 14.5 ns. The pulses induced by gamma-rays were also found in this FW1/4PH region without any PSD processing, although it was completely excluded after PSD processing with R. This result indicates that the combination of R and FW1/4PH can discriminate between pulses induced by alpha and gamma irradiation. Indeed, the R of the pulses with a FW1/4PH region of 11.5 - 14.5 ns added in Fig. 2 showed that the pulses induced by gamma-ray irradiation was sufficiently eliminated.

Figures 4 exhibit deposited energy spectra for pulses in the SDD with a ^{6}LiF thermal neutron converter and without one irradiated in the UTR-KINKI reactor. The reactor power in these measurements were 1 W. The deposited energy was calibrated using a ^{241}Am source. The spectra were clearly different in these two cases. In the case of the SDD without the thermal neutron converter, the spectrum for total pulse (the pulse data without PSD processing) had a peak at around 0.5 MeV, and showed a gradual decrease in the event rate with increasing deposited energy up to 6 MeV. After the PSD with R and FW1/4PH, the peak energy slightly decreased to 0.7 MeV. According to the PSD method and the absence of the thermal neutron converter, the spectrum after this PSD processing should be induced only by fast neutron. Indeed, the fact that the neutron energy spectrum extends to above 5 MeV roughly agreed to the expected neutron spectrum in the core region of the UTR-KINKI reactor [15].

The spectra of the SDD with a ^{6}LiF thermal neutron converter were clearly different. The spectrum for total pulse showed two peaks at 0.5 and 2.8 MeV. Then the first peak decreased after the PSD with only R. Finally, the PSD method using R and FW1/4PH unveiled a peak at 1.2 MeV. The count rate in the peak at 2.8 MeV did not change in
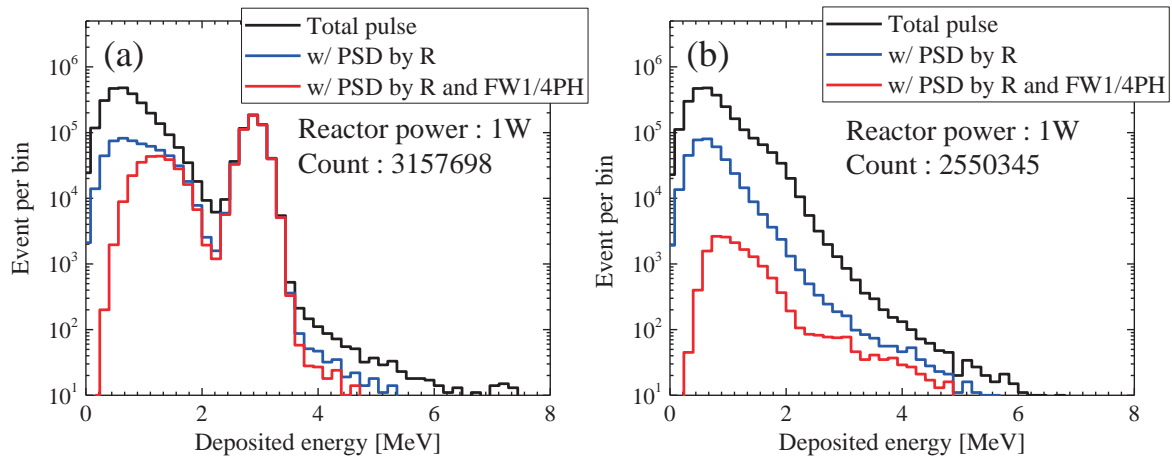

Fig. 3 Histogram of FW1/4PH by (a) alpha-ray and (b) gamma-ray irradiation for pulses without PSD processing and pulses with rectangular shape ($R > 0.6$).

Fig. 4 Energy deposition spectra for (a) SDD with ^{6}LiF thermal neutron converter and (b) SDD without 6LiF thermal neutron converter irradiated at the core region of the UTR-KINKI reactor. Total pulse (black line) here indicates all pulse data without PSD processing. Data after PSD processing using R and both R and *FW1/4PH* are also displayed as blue and red lines, respectively.

this processing. The deposition energy of 2.8 MeV was consistent with the primitive recoil energy of triton generated in ^{6}Li(n,α)^{3}H reaction. The other peak observed at 1.2 MeV should be attributed to alpha particles produced in ^{6}Li(n,α)^{3}H reaction, although the recoil energy of alpha particles in this reaction is about 2.0 MeV. This lowered deposition energy of alpha particles would be caused by the over-subtraction of the pulse height by the background current in data acquisition system in the background subtraction process. Also, because of the larger positive charge and the mass of alpha particle, the energy loss of alpha particle is larger than that of triton, resulting in the lower count rate for alpha particles than that for tritons. By these attributions, it was found that the peak by alpha particles was successfully extracted from the pulses induced by gamma-rays and fast neutrons by the PSD method. Additionally, the count rate in the triton peak lost in the PSD processing was less than 3%, indicating that an effective PSD method was achieved.

The extracted pulses by the PSD method in the SDD with the ^{6}LiF thermal neutron converter should be mixed with pulses by the energetic alpha, triton and fast neutron particles, although that without the thermal neutron converter counted only fast neutrons. The subtraction of the extracted spectra in the SDD with and without the thermal neutron converter can deduce the spectrum only by the energetic charged particles induced by thermal neutrons. The deduced spectra normalized by the reactor power are displayed in Fig. 5 to evaluate the dependency of the count rate of the energetic charged particles on the reactor power, which should be correlated with thermal neutron flux. As found in Fig. 5, the count rate was linearly proportional to the reactor power. The thermal neutron flux in the core region of the UTR-KINKI reactor was estimated using the detection efficiency evaluated in our previous study [22] as 7.6×10^6 n cm^{-2} s^{-1} at the reactor power of 1 W. The evaluated flux was almost consistent with the actual thermal
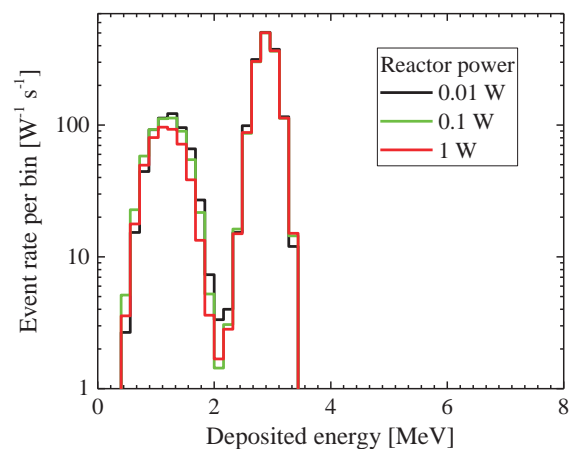

Fig. 5 Count rates of energetic charged particles for the SDD with ^{6}LiF thermal neutron convertor. Count rates are normalized by the reactor power.

neutron flux measurement using gold foil [23, 24]. This result strongly indicates the validity of the present analysis using the SDD and the developed PSD method.

4. Conclusion

This study established a PSD method for the SDD to extract wide and rectangular shaped pulses which are induced by fast neutron and energetic charged particles and accordingly to reject the pulses induced by gamma-rays. Additionally, the use or absence of a thermal neutron converter in the SDD can deliver the count rate only by the energetic charged particles induced by thermal neutrons. A reliable thermal neutron flux measurement procedure applicable for fusion reactor development was achieved in this work.

A good linearity in the count rate for energetic charged particles was obtained up to the thermal neutron flux of

7.6×10^6 n cm^{-2} s^{-1} in this study. The capability of this detector and the developed PSD method in the higher flux field will be investigated in future.

Acknowledgements

[1] M. Nocente *et al.*, Fast ion energy distribution from third harmonic radio frequency heating measured with a single crystal diamond detector at the Joint European Torus, Rev. Sci. Instrum. **86**, 103501 (2015).

[2] D. Rigamonti *et al.*, Neutron spectroscopy measurements of 14 MeV neutrons at unprecedented energy resolution and implications for deuterium tritium fusion plasma diagnostics, Meas. Sci. Technol. **29**, 4 (2018).

[3] C. Cazzaniga *et al.*, Single crystal diamond detector measurements of deuterium-deuterium and deuterium-tritium neutrons in Joint European Torus fusion plasmas, Rev. Sci. Instrum. **85**, 043506 (2014).

[4] C. Cazzaniga *et al.*, A diamond based neutron spectrometer for diagnostics of deuterium-tritium fusion plasmas, Rev. Sci. Instrum. **85**, 11E101 (2014).

[5] L. Giacomelli *et al.*, Neutron emission spectroscopy of DT plasmas at enhanced energy resolution with diamond detectors, Rev. Sci. Instrum. **87**, 11D822 (2016).

[6] M. Rebai *et al.*, Pixelated Single-crystal Diamond Detector for fast neutron measurements, J. Instrum. **10**, C03016 (2015).

[7] A. Muraro *et al.*, First neutron spectroscopy measurements with a pixelated diamond detector at JET, Rev. Sci. Instrum. **87**, 11D833 (2016).

[8] T. Du, X. Peng, Z. Chen, Z. Hu, L. Ge, L. Hu, G. Zhong, N. Pu, J. Chen and T. Fan, Time Dependent DD Neutrons Measurement Using a Single Crystal Chemical Vapor Deposition Diamond Detector on EAST, Plasma Sci. Technol. **18**, 950 (2016).

[9] X. Xie, X. Yuan, X. Zhang, Z. Chen, X. Peng, T. Du, T. Li, Z. Hu, Z. Cui, J. Chen, X. Li, G. Zhang, T. Fan, G. Yuan, J. Yang and Q. Yang, Application of a single crystal chemical vapor deposition diamond detector for deuteron plasma neutron measurement, Nucl. Instrum. Methods Phys. Res. A **761**, 28 (2014).

[10] M. Kobayashi, K. Ogawa, M. Isobe, T. Nishitani, S. Kamio, Y. Fujiwara, T. Tsubouchi, S. Yoshihashi, A. Uritani, M. Sakama, M. Osakabe and the LHD Experiment Group, Thermal neutron flux evaluation by a single crystal CVD diamond detector in LHD deuterium experiment, J. Instrum. **14**, C09039 (2019).

[11] P. Kavrigin, P. Finocchiaro, E. Griesmayer, E. Jericha, A. Pappalardo and C. Weiss, Pulse-shape analysis for gamma background rejection in thermalneutron radiation using CVD diamond detectors, Nucl. Instrum. Methods Phys. Res. A **795**, 88 (2015).

[12] M.I. Kobayashi, M. Angelone, S. Yoshihashi, K. Ogawa, M. Isobe, T. Nishitani, S. Sangaroon, S. Kamio, Y. Fujiwara, T. Tsubouchi, A. Uritani, M. Sakama, M. Osakabe and the LHD Experiment Group, Thermal neutron measurement by single crystal CVD diamond detector applied with the pulse shape discrimination during deuterium plasma experiment in LHD, Fusion Eng. Des. **161**, 112063 (2020).

[13] UTR-KINKI research reactor of the KINDAI University, Japan https://www.kindai.ac.jp/files/rd/research-center/aeri/guide/external-use/outside4.pdf (in Japanese)

[14] S. Endo, T. Taniguchi, T. Kajimoto, K. Tanaka, M. Takada, S. Kamada, T. Horiguchi and K. Fujikawa, Measurement of the gamma-ray energy spectrum of the educational Kinki University Reactor (UTR-KINKI), Appl. Rad. Isotopes **124**, 90 (2017).

[15] S. Endo, K. Tanaka, K. Fujikawa, T. Horiguchi, T. Itoh, G. Bengua, T. Nomura and M. Hoshi, Distortion of neutron field during mice irradiation at Kinki University Reactor UTR-KINKI, Appl. Rad. Isotopes **65**, 1037 (2007).

[16] W. Shockley, Currents to Conductors Induced by a Moving Point Charge, J. Appl. Phys. **9**, 635 (1938).

[17] Z. He, Review of the Shockley–Ramo theorem and its application in semiconductor gamma-ray detectors, Nucl. Instrum. Methods Phys. Res. A **463**, 250 (2001).

[18] T. Williams, C. N'Diaye, D. Breton, K. Cassou, K. Dupraz, P. Favier, D. Jehanno, V. Kubytskyi, X. Liu, J. Maalmi, A. Martens, Y. Peinaud, A. Stocchi, F. Zomer, E. Griesmayer, P. Kavrigin, M.W. Ahmed, M. Sikora and H.R. Weller, Operation of a fast diamond γ-ray detector at the HIγS facility, Nucl. Instrum. Methods Phys. Res. A **830**, 391 (2016).

[19] C. Weiss, H. Frais-Kolbl E. Griesmayer and P. Kavrigin, Ionization signals from diamond detectors in fast-neutron fields, Eur. Phys. J. A **52**, 269 (2016).

[20] https://cividec.at

[21] K. Ogawa, M. Isobe, T. Nishitani and T. Kobuchi, The large helical device vertical neutron camera operating in the MHz counting rate range, Rev. Sci. Instrum. **89**, 113509 (2018).

[22] M.I. Kobayashi, S. Yoshihashi, K. Ogawa, M. Isobe, S. Sangaroon, S. Kamio, Y. Fujiwara and M. Osakabe, A comprehensive evaluation of the thermal neutron detection efficiency by single crystal CVD diamond detector with LiF thermal neutron converter, Fusion Eng. Des. **179**, 113117 (2022).

[23] A. Kitamura, J. Matsumoto, Y. Furuyama, A. Taniike, N. Kubota, T. Ohsawa, K. Hashimoto, T. Horiguchi and T. Tsuruta, Measurements and Analysis of Neutron Flux Distribution in UTR-KINKI, J. Nucl. Sci. Technol. **40**, 349 (2003).

[24] K. Kobayashi, T. Yoshimoto, Z. Li, I. Kimura, S. Kanazawa and T. Ohsawa, Determination of thermal and intermediate neutron spectrum at UTR-KINKI using Cf-ratio measurement by activation method, Report of Cooperative Research Using UTR-KINKI, Fac. of Eng., Osaka Univ. **35**, 15 (1999).